

Submm p-Ge Laser using a Regular Permanent Magnet

Kijun Park, Jin J. Kim, and Robert E. Peale

Center for Research and Education in Optics and Lasers (CREOL),
University of Central Florida, Orlando, Florida 32816-2700

Henry Weidner

Department of Physics, University of Central Florida

Kijun Park and Jin J. Kim are also with the Department of Electrical and Computer Engineering.
Jin J. Kim and Robert E. Peale are also with the Department of Physics

E. E. Haller

Lawrence Berkeley Laboratory, University of California, Berkeley, California 94720

Abstract

We have demonstrated a novel p-Ge laser at 100 μm wavelengths in Voigt configuration using a *regular permanent magnet* instead of a superconducting one. The temperature dependence of emission below 4.2 K is reported for the first time, along with a study of free space beam characteristics, of output couplers, and of repetition rate.

Introduction

We report emission near 100 μm from a table-top semiconductor laser based on sub-mm transitions from light to heavy hole bands in p-Ge. This lasing mechanism has been studied for a number of years outside the USA [1]. Our new idea, reported here, is to substitute a regular permanent magnet for the traditional superconducting magnet. It also provides an easier setup for the favorable Voigt configuration. This new system has potential for many practical applications.

The submm (or far-infrared) region has long been without adequate tunable laser sources. Potential applications of such a source include plasma diagnostics, satellite communications, remote sensing, molecular and solid state spectroscopy, particle sizing, and laser velocimetry. Free electron lasers operate in the 100 μm region, but these are large, expensive facilities. The p-Ge laser appears to be the most promising source to date. First demonstrated in Russia and Japan more than a decade ago [2, 3], this paper and an upcoming paper by Coleman and Wierer [4] are the

first reports of experimental activity on this subject in this hemisphere.

A p-Ge laser is based on population inversion between light and heavy hole bands. Fig. 1 shows these bands vs. wavevector and qualitatively explains the basic principles of operation [1]. An electric field accelerates holes perpendicular to a magnetic field. Population inversion is achieved when E/B is tuned to prevent light holes from reaching the threshold for inelastic optical phonon scattering while allowing heavy holes to do so. Light holes remain "hot," while heavy holes scatter back to $k = 0$ and some end up in the light hole band, establishing population inversion.

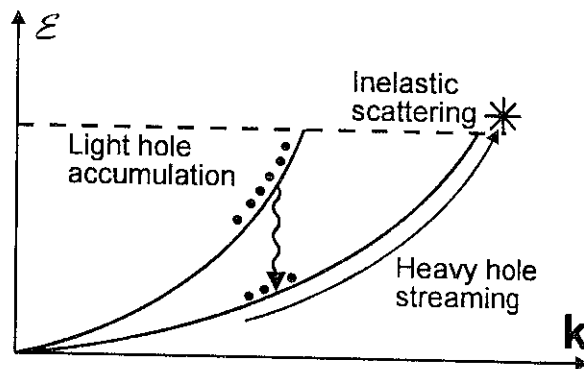


Figure 1. Light and heavy hole energies vs. wavevector. The dashed line shows the threshold for inelastic optical phonon scattering.

The laser wavelength is tunable over the broad gain region in k -space by use of a selective external resonator. The gain region is homogeneously broadened [5], so all the population inversion is

available for emission at any wavelength selected. So far, almost all studies have been carried out in the Faraday configuration, which is not necessarily optimum for the oscillations on inter-valence band transitions in p-Ge [6, 7]. Emission from Voigt configured p-Ge has been observed to be several times stronger than that from the Faraday configured one [7].

Two basic approaches have been followed in this work. The first has been to construct a device using the traditional superconducting magnet in Faraday geometry for variable B-field studies and to make connection to previous work. Our second and new approach has been to substitute a regular high-field permanent magnet for the traditional superconducting magnet. Though the crystal must still be cooled, the absence of superconducting coils eliminates the need for liquid helium.

General Experimental Details

A rectangular bar of p-Ge with Ga concentration of $3 \times 10^{14} \text{ cm}^{-3}$ (grown at Berkeley) is used, though this is on the high side of the acceptable range. The bar is placed inside the superconducting magnet or between the poles of the permanent magnet. The crystal was oriented so that $\mathbf{B} \parallel [001]$ for the Voigt configuration and $\mathbf{B} \parallel [110]$ for the Faraday configuration. Current pulses (120 ~ 650 A) of $\sim 1 \mu\text{s}$ duration were applied at 1 to 100 Hz through Ohmic contacts on the $[1-10]$ faces.

The end surfaces of the Ge rod were polished parallel to better than 1 arc-min as tested using HeNe laser reflections. The other sides were rough ground to prevent feedback of non-axial modes. We used a polished copper back mirror. A Cu-mirror with a 1-mm hole or a metal mesh was used as the output coupler. The free standing metal mesh was #500 (stainless steel, period = $50 \mu\text{m}$) or #1000 (Ni, period = $25 \mu\text{m}$), and was insulated from the Ge by a thin PTFE foil. Reflectance of each mesh was calculated and its transmittance was measured using a Fourier transform spectrometer [8, 9].

Each magnet design is fastened to the end of an insert for a variable temperature (2 ~ 300 K) cryostat with ZnSe inner windows and polyethylene outer windows. The radiation is collected by a gold-coated off-axis ellipsoidal mirror focused onto a 4 K Si bolometer, whose signal was processed by a boxcar averager. The temperature was determined using a calibrated 1 k Ω resistor mounted directly in contact with the Ge crystal. Fig. 2 presents the transmission of radiation from a global source through the 2 K ZnSe and 300 K polyethylene windows measured using the Fourier spectrometer and bolometer. The broad zero

below $70 \mu\text{m}$ is due to phonon absorption in ZnSe. The long-wavelength falloff is due to the spectral response of the detector, the $12 \mu\text{m}$ pellicle beamsplitter, and the source. This spectrum demonstrates that the windows and the detector are well suited to transmit and detect p-Ge laser emission near $100 \mu\text{m}$. In our experiments a $100 \mu\text{m}$ long pass filter was used, and since the bolometer responsivity is very low beyond about $250 \mu\text{m}$, no emission outside the $100 \sim 250 \mu\text{m}$ range is detected.

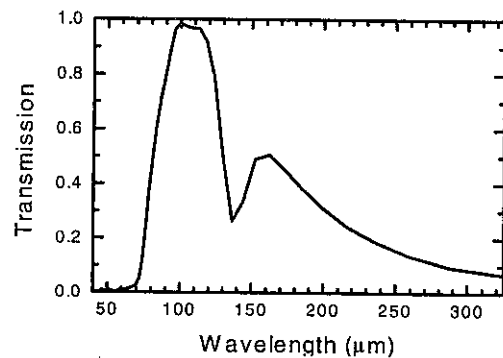


Figure 2. Transmission spectrum of 2 K ZnSe and 300 K polyethylene.

Faraday configuration using a superconducting magnet

Fig. 3 shows a scale diagram of the radiation detection system and the superconducting magnet insert with the p-Ge inside the solenoid. The device is clearly compact. We used a polished brass mirror to reflect the emission horizontally out of the cryostat chamber.

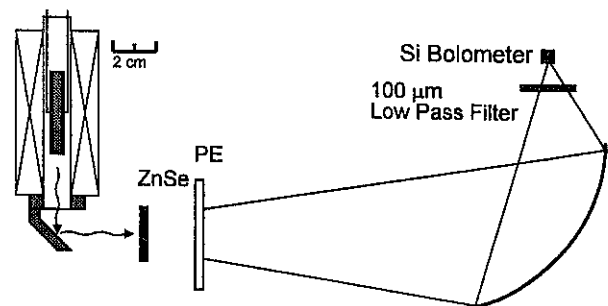


Figure 3. Schematic of the experimental set-up for the Faraday configured p-Ge in a superconducting magnet.

Emission from a $4 \times 5 \times 40 \text{ mm}^3$ p-Ge rod in the Faraday-configured superconducting magnet is shown

as a function of E and B in Fig. 4. A mirror made of electro-plated Cu on a Ge plate with a 1-mm-diam hole was used as the output coupler. Emission is observed when $E = 0.5 \sim 1.4$ kV/cm and $B = 0.7 \sim 1.3$ T, a limited range of E/B as predicted by semiclassical theory and observed by several groups [1].

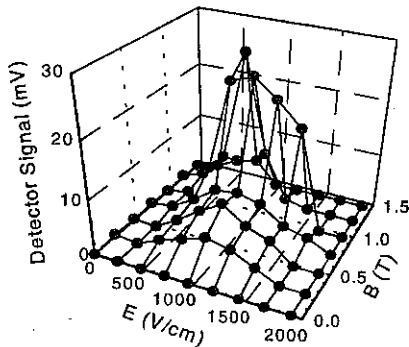


Figure 4. Measured signal as a function of E and B for a p-Ge laser in Faraday configuration using a superconducting magnet.

Voigt configuration using a permanent magnet

Our permanent magnet system shown in Fig. 5 is made of 35 MG-Oe NdFeB alloy and soft iron. The yoke and the poles, made of soft iron, are designed to concentrate magnetic flux through the Ge. Fig. 5 also shows the calculated field between the poles. Our optimized design provides a uniform field between the poles as determined by both a finite element analysis and measurement, which shows that the magnetic field in the sample volume is uniform within 3%. A $3.5 \times 3.9 \times 25$ mm³ p-Ge rod is placed between the magnet poles, and the whole system is placed in the cryostat.

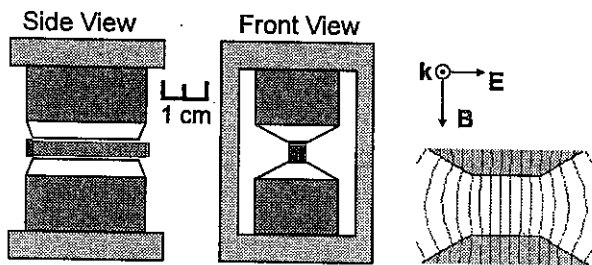


Figure 5. Schematic of the Voigt configured permanent magnet laser design. For the field-line plot, the directions of the magnetic field, the electric-field applied to the sample, and the propagation vector of the emission are shown.

The emission from p-Ge is shown as a function of applied electric field in Fig. 6 for different output coupling. The open circles show emission with a #1000 mesh output coupler ($R \sim 99\%$). The filled circles show the emission without an output coupler. Several effects are observed. Higher output-coupler reflectivity reduces the threshold for emission. The emission intensity saturates above some E-field even though we observe that the current density increases linearly as the applied voltage is increased. Intensity saturation is observed at different electric fields, depending upon the reflectivity of the front surface. For both curves the emission is observed to higher electric-fields than in Faraday configuration, i. e. > 2.5 kV/cm for Voigt configuration vs. 1.2 kV/cm for Faraday configuration.

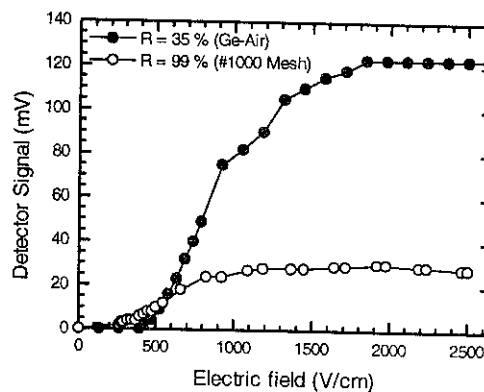


Figure 6. Measured signal as a function of electric field for a p-Ge rod in the Voigt configuration.

A lower output intensity for 99% reflectivity than for the 35% reflectivity provided by the bare Ge surface suggests that the optimum output coupling may be somewhere in between. In order to explore this dependence, we plot in Fig. 7 the maximum intensity at $E = 1.9$ kV/cm vs. reflectivity for different output coupling, including data from earlier experiments with unoptimized polishing. (By coating the front surface with a 20 μ m thick PTFE without an output coupler, reflectivity of $\sim 23\%$ is achieved. A $\sim 90\%$ reflectivity is achieved using #500 mesh.) These preliminary results suggest an optimum reflectivity of about 50%. More systematic studies are in progress.

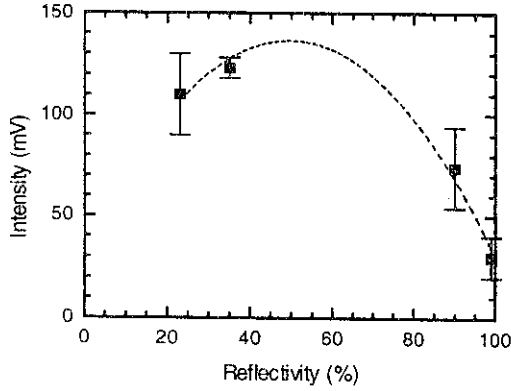


Figure 7. Maximum intensity vs. output coupler reflectivity at $E = 1.9$ kV/cm and $T \sim 4$ K. The dashed line is a guide to the eye.

The beam profile of the emission from the Voigt configured laser without an output coupler ($R = 35\%$) is shown in Fig. 8. The points were determined by blocking the beam with a straight-edged shutter at 80 mm from the face of the p-Ge. The curve is a fit assuming a Gaussian intensity profile. The divergence of the beam is smaller than the $f/4$ collection cone of the bolometer system.

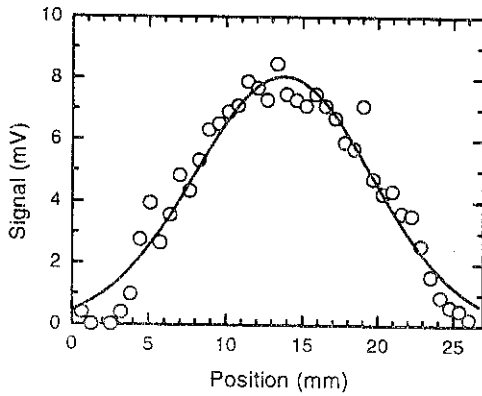


Figure 8. Beam profile without an output coupler ($R = 35\%$) at distance of 80 mm from the source at $E = 1.3$ kV/cm and sample temperature = 4.5 K.

The variable temperature cryostat allows studies of the temperature dependence of the emission down to 1.7 K, as shown in Fig. 9. The peak occurs at around 3 ~ 8 K. Experiments below 4.2 K have not been previously reported. We observe a decrease in signal below 3 K. Our tentative model involves strain splitting of the valence band at $k = 0$ so that a small amount of

thermal energy is required for holes to enter the light hole band. This suggests that externally applied stress could serve to increase the temperature range for observing laser emission.

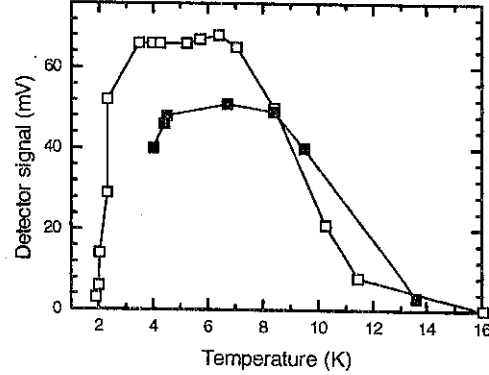


Figure 9. Measured signal as a function of temperature at 1.6 kV/cm (open square) and 1.1 kV/cm (filled square).

Fig. 10 shows the emission intensity vs. repetition rate. For superconducting magnet designs the maximum repetition rate is usually observed to be less than several Hz [1]. However, we have observed no significant decrease in emission up to 50 Hz when using our permanent magnet, whose open design facilitates cooling. Above 50 Hz, the phonons created by heating destroy the anisotropic momentum distribution required for the emission.

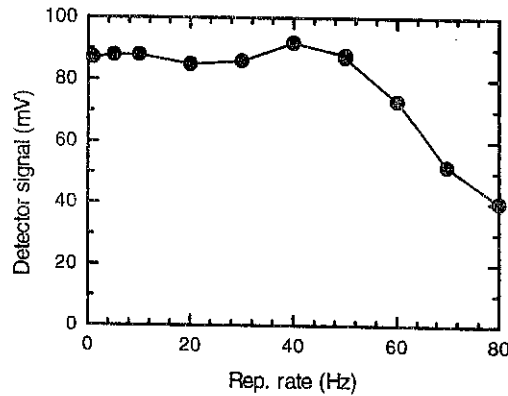


Figure 10. Measured signal strength vs. repetition rate without an output coupler at $E = 1.05$ kV/cm in Voigt configuration.

Summary

We have demonstrated a novel p-Ge laser using a regular permanent magnet. An output coupler reflectivity of around 50 % appears to be optimum at ~4 K. We measured the temperature dependence of emission below 4.2 K for the first time and observed a dramatic decrease in signal below 3 K. Our measurement of the free space beam profile reveals a Gaussian intensity distribution. Repetition rates up to 50 Hz are possible because of the efficient cooling enabled by the permanent magnet design.

To date, all studies of submm lasing in p-Ge have been performed with superconducting magnets immersed in liquid helium. This obviously handicaps the ultimate utility of the device. Our observation of submm emission from a Voigt-configured p-Ge laser using a regular permanent magnet represents a breakthrough in practicality because it considerably simplifies the device and eliminates the necessity of liquid helium.

Acknowledgments

This work was supported in part by internal funds provided by CREOL. REP thanks AFOSR and University of Central Florida Division of Sponsored Research for support.

References

1. See, for example, *Optical and Quantum Electronics* Volume 23 (1991) for a comprehensive review.
2. S. Komiyama, "Far-infrared emission from population-inverted hot-carrier systems in p-Ge," *Phys. Rev Lett.* **48**, 271 (1982).
3. A. A. Andronov, I. V. Zverev, V. A. Kozlov, Yu. N. Nozdrin, S. A. Pavlov, and V. N. Shastin, "Stimulated emission in the long-wavelength IR region from hot holes in Ge in crossed electric and magnetic fields," *JETP Lett.* **40**, 804 (1984).
4. Paul D. Coleman and Jonathan Wierer, "Establishment of a dynamic model for the p-Ge far IR laser," *Int. J. Infrared and Millimeter Waves*, to be published.
5. Fritz Keilmann and Hanna Zuckermann, "Transient gain of the germanium hot hole laser," *Opt. Commun.* **109**, 296 (1994).
6. Iwao Hosako and Susumu Komiyama, "p-type Ge far-infrared laser oscillation in Voigt configuration," *Semicond. Sci. Technol.* **7**, B645 (1992).
7. L. E. Vorobjev, S. N. Danilov, D. V. Donetsky, D. A. Firsov, Yu. V. Kochegarov, V. I. Stafeev, "An injectionless FIR laser based on interband transitions of hot holes in germanium," *Semicond. Sci. Technol.* **9**, 641 (1994).
8. Lewis B. Whitbourn and Richard C. Compton, "Equivalent-circuit formulas for metal grid reflectors at a dielectric boundary," *Appl. Opt.* **24**, 217 (1985).
9. R. C. Compton, L. B. Whitbourn, and R. C. McPhedran, "Strip gratings at dielectric interface and application of Babinet's principle," *Appl. Opt.* **23**, 3236 (1984).